AIMS Mathematics, 10(2): 3227–3250.
DOI: 10.3934/math.2025150
Received: 08 December 2024
Revised: 25 January 2025
Accepted: 14 February 2025
Published: 20 February 2025

https://www.aimspress.com/journal/Math

Research article

Analysis and anti-control of period-doubling bifurcation for the one-dimensional discrete system with three parameters and a square term

Limei Liu* and Xitong Zhong

College of Applied Mathematics, Jilin University of Finance and Economics, Changchun 130117, China

* **Correspondence:** Email: 109021@jlufe.edu.cn.

Abstract: In certain nonlinear systems, period-doubling bifurcations are a common way to cause chaos. Additionally, bifurcation advance or delay can be realized using anti-control of period-doubling bifurcation. To address the practical needs of engineering, anti-control of period-doubling bifurcation is a typical method of applying chaos. Based on these reasons, we conducted the following research: First, we proposed a new one-dimensional discrete system with three parameters and a square term. Existence and stability at the fixed point were studied for the one-dimensional discrete system with three parameters and a square term. Furthermore, bifurcation theory was used to determine the conditions of existence for transcritical bifurcation and period-doubling bifurcation. Numerical experiments verified the theoretical assessments of the bifurcation's results. Then, the state linear feedback control approach was used to implement the anti-control of period-doubling bifurcation in order to realize period-doubling bifurcation advance for the one-dimensional discrete system with three parameters and a square term. The conditions of the appropriate control parameters were analyzed in theory. Numerical experiments confirmed the efficiency and robustness of anti-control of period-doubling bifurcation for the one-dimensional discrete system with three parameters and a square term. The one-dimensional discrete system with three parameters and a square term with the anti-controller has advantages in image encryption.

Keywords: anti-control; period-doubling bifurcation; stability analysis; one-dimensional discrete system with three parameters and a square term; chaos; image encryption
Mathematics Subject Classification: 39A28, 39A30, 39A33, 65P30, 93B52

1. Introduction

The chaotic system has a high sensitivity to the initial condition and random-alike appearance, so it shows erratic, aperiodic, and nonlinear phenomena easily. Some of these phenomena are investigated by researching dynamical behaviors such as stability, bifurcations, and chaos [1]; some are investigated by explaining the formation and overall structure of strange attractors [2]; some are studied with computational simulations for Lyapunov exponent [3], time series analysis, and cobweb representation [4]. The erratic, aperiodic, and nonlinear phenomena can be used in many branches of society and nature; thus, many researchers are attracted to investigate the chaotic systems. Chaotic maps have emerged as a primary focus of research. Chaotic maps are the iterative functions in dynamical systems that display chaotic behavior. They are susceptible to the system's specifications and starting circumstances. They are applied in various fields, which attract the attention of researchers to construct chaotic maps and investigate chaotic behaviors [5–9]. The constructed chaotic maps encompass one-dimension maps, two-dimension maps, and high-dimension maps [10–12]. Among these maps, one-dimensional chaotic maps are a fascinating subject because of their good chaotic qualities and simple structure, making them the most feasible of these maps to implement. One of the well-known chaotic maps is the logistic map, which is defined by

$$x_{n+1} = \mu x_n(1-x_n), \quad n = 0,1,2,\ldots, \tag{1}$$

where $\mu > 0$, $x_n \in [0,1]$. In 1976, May demonstrated that logistic maps may display complicated chaotic behaviors [13]. Following May's work, a large number of one-dimensional chaotic maps are discovered that, for certain parameters with straightforward equations, show chaotic behavior, such as the Tent Map, Sine Map [14], one-dimensional cosine within sine chaotic map [15], and the one-dimensional quadratic map [16]. Among these maps, the structure of the one-dimensional chaotic map K [4] is the most similar to the one-dimensional logistic map, which is defined by

$$x_{n+1} = K(x_n) = \frac{\mu x_n(1-x_n)}{1+x_n}, \quad n = 0,1,2,\ldots, \tag{2}$$

where $\mu > 0$, $x_n \in [0,1]$. Furthermore, compared to a one-dimensional logistic map, the range of chaos and stability in a one-dimensional chaotic map K is greater. One-dimensional logistic map and one-dimensional chaotic map K both belong to one-dimensional discrete systems where the denominator is a linear function and the numerator is a quadratic function. Due to its unique mathematical properties, this type of discrete system has a wide range of applications in various fields, including in economics and finance, in mechanics and vibration analysis, in biology, in signal processing and control systems, in algorithm analysis and data structures, in chaos theory, in optimization problems, and in the field of education and testing. These applications demonstrate the diversity and importance of the one-dimensional discrete system with a linear denominator and a quadratic numerator. Thus, the one-dimensional discrete system with three parameters and a square term is proposed and further studied in this paper, which can be defined as a one-dimensional discrete system with a linear denominator and a quadratic numerator. Through a one-dimensional discrete system with three parameters and a square term, we can better understand and predict the behavior of complex systems and find optimal solutions to practical problems.

Though one-dimensional chaotic maps are advantageous because of their straightforward design and ease of use, the complexity and security of one-dimensional chaotic maps are considered. In order to increase the range of stability and the chaotic behavior, control technology is crucial. Most

researchers contribute to controlling chaos and bifurcations [17,18]. Since the occurrences of bifurcations may cause chaos, sometimes the controllers are designed to make the bifurcations appear in advance. These controllers are called the anti-control of bifurcations, which is the inverse process of the bifurcation control. The anti-control method is theoretically straightforward and efficient [19]. It satisfies the practical requirements of engineering applications by enabling the system to accomplish the required bifurcation phenomena at any critical value [20]. As period-doubling bifurcation may cause chaos, a few researchers have been interested in the anti-control on period-doubling bifurcation [21]. The researchers in [22] carried out anti-control of multiplicative period bifurcations for one-dimensional logistic systems using feedback control methods to set up nonlinear controllers for the purpose of anti-control of period multiplicative bifurcations that are divided into two. It aims to manage the period-doubling bifurcations and lower the higher stable 2n-periodic orbit of the system to be controlled to lower stable 2m-periodic orbits (m<n). In this paper, in order to increase the complexity of chaos, anti-control of period-doubling bifurcation is designed to make the one-dimensional discrete system with three parameters and a square term to generate the period-doubling bifurcation at a predetermined position.

The remainder of this paper is structured as follows: The one-dimensional discrete system with three parameters and a square term is described in Section 2, and the existence and stability of its fixed points are studied. The bifurcation behaviors of the one-dimensional discrete system with three parameters and a square term are analyzed theoretically and numerically in Section 2. Using bifurcation theory, we demonstrate the existence of transcritical bifurcation and period-doubling bifurcation. We derive conditions for transcritical bifurcation and period-doubling bifurcation. In Section 3, the state linear feedback control approach is used to create the anti-control of the period-doubling bifurcation for the one-dimensional discrete system with three parameters and a square term. Numerical experiments are used to verify the effectiveness and robustness of the anti-control of the period-doubling bifurcation for the one-dimensional discrete system with three parameters and a square term. An image encryption experiment is carried out for the one-dimensional discrete system with three parameters and a square term with an anti-controller. Our major conclusions are outlined in Section 4.

2. Stability and bifurcation of the fixed points of the one-dimensional discrete system with three parameters and a square term

2.1. Existence and stability of the fixed points

Consider the one-dimensional discrete system with three parameters and a square term $f:[0,1]\to[0,1]$, which is defined as

$$x_{n+1}=f\left(x_n\right)=\frac{\mu x_n(1-x_n)}{a+bx_n},\quad n=0,1,2,\ldots, \tag{3}$$

where $\mu>0$, $a>0$, $b\geq 0$, $x_n\in[0,1]$. The one-dimensional discrete system with three parameters and a square term (1) is called the Smith-like population growth model. The meaning and function of x_n, μ, a, b are similar to the parameters in the Smith's population growth model [23]. x_n is similar to the number of populations, and n represents the number of iterations. μ is similar to population fertility. a is similar to the maximum population size that the environment can sustain. b

is similar to the impact of population density on resource availability. The one-dimensional discrete system with three parameters and a square term (1) can be used in many fields, such as biological population study, ecosystem dynamic analysis, population policy formulation reference, market trend analysis, resource management and allocation, and epidemic prevention and control.

The one-dimensional discrete system with three parameters and a square term (3) can be rewritten as

$$x \mapsto f(x) = \frac{\mu x(1-x)}{a+bx}, \tag{4}$$

where $\mu > 0, a > 0, b \geq 0, x \in [0,1]$.

The fixed points of the one-dimensional discrete system with three parameters and a square term (3) satisfy the following equation

$$x^* = \frac{\mu x^*(1-x^*)}{a+bx^*}. \tag{5}$$

By a simple analysis, the following propositions are obtained.

Proposition 1. *(a) If* $\mu \leq a$, *the one-dimensional discrete system with three parameters and a square term* (3) *has the unique fixed point* $x^* = 0$; *(b) if* $\mu > a$, *the one-dimensional discrete system with three parameters and a square term* (3) *has two fixed points*:

$$x_1^* = 0, \quad x_2^* = \frac{\mu - a}{\mu + b}.$$

Proof of Proposition 1. The solutions of equation

$$x^* = \frac{\mu x^*(1-x^*)}{a+bx^*}$$

are

$$x^* = 0 \text{ and } x^* = \frac{\mu - a}{\mu + b}.$$

a) If $\mu \leq a$, then

$$x^* = \frac{\mu - a}{\mu + b} \leq 0.$$

However, the one-dimensional discrete system with three parameters and a square term (3) shows that $x^* \in [0,1]$; thus, $x^* = 0$ is a unique solution of Eq (5). Thus, if $\mu \leq a$, the one-dimensional discrete system with three parameters and a square term (3) has a unique fixed point $x^* = 0$.

b) If $\mu > a$, then

$$1 \geq x^* = \frac{\mu - a}{\mu + b} > 0.$$

$$x^* = 0 \text{ and } x^* = \frac{\mu - a}{\mu + b}$$

are the solutions of Eq (5). Thus, if $\mu > a$, the one-dimensional discrete system with three parameters and a square term (3) has two fixed points:

$$x_1^* = 0 \text{ and } x_2^* = \frac{\mu - a}{\mu + b}.$$

This completes the proof.

In order to study the stability of the fixed points of one-dimensional discrete system with three parameters and a square term (3), a very small displacement δx_n is set at the fixed points x^*, namely

$$\delta x_n = x_n - x^*,$$

the one-dimensional discrete system with three parameters and a square term (3) can be rewritten as

$$x^* + \delta x_{n+1} = f(x^* + \delta x_n). \tag{6}$$

The Taylor expansion of map (6) is simplified as

$$\delta x_{n+1} = f'(x^*)\delta x_n + \ldots, \tag{7}$$

where

$$f'(x) = \frac{a\mu - 2a\mu x - b\mu x^2}{(a + bx)^2}.$$

When $|f'(x^*)| > 1$, $|\delta x_{n+1}|$ is larger than $|\delta x_n|$, which means the displacement from the fixed point is increasing, so the fixed point is unstable.

When $|f'(x^*)| < 1$, $|\delta x_{n+1}|$ is smaller than $|\delta x_n|$, which means the displacement from the fixed point is decreasing, then the fixed point is stable.

According to the above analysis, the stability of the fixed points of the one-dimensional discrete system with three parameters and a square term (3) satisfies Theorem 1.

Theorem 1. *Considering the one-dimensional discrete system with three parameters and a square term* (3), *the stability of the fixed points is listed as follows*:

$$\textit{The fixed point } x^* = 0 \textit{ is} \begin{cases} \textit{stable}, & 0 < \mu < a, \\ \textit{unstable}, & \mu > a. \end{cases}$$

$$\textit{The fixed point } x^* = \frac{\mu - a}{\mu + b} \textit{ is} \begin{cases} \textit{stable}, & a < \mu < \dfrac{3a + b + \sqrt{(9a + b)(a + b)}}{2}, \\ \textit{unstable}, & \mu > \dfrac{3a + b + \sqrt{(9a + b)(a + b)}}{2}. \end{cases}$$

Proof of Theorem 1. When the fixed point is

$$x^* = 0, \quad f'(0) = \frac{\mu}{a}.$$

If

$$0 < \mu < a, \ \left| f'(0) \right| = \frac{\mu}{a} < 1,$$

then the unique fixed point $x^* = 0$ is stable; if

$$\mu > a, \ \left| f'(0) \right| = \frac{\mu}{a} > 1,$$

the fixed point $x^* = 0$ is unstable.

When the fixed point is

$$x^* = \frac{\mu - a}{\mu + b}, \quad f'\left(\frac{\mu - a}{\mu + b} \right) = \frac{ab + 2a\mu - \mu^2}{(a+b)\mu}.$$

If

$$a < \mu < \frac{3a + b + \sqrt{(9a+b)(a+b)}}{2}, \ \left| f'\left(\frac{\mu - a}{\mu + b} \right) \right| = \left| \frac{ab + 2a\mu - \mu^2}{(a+b)\mu} \right| < 1,$$

the fixed point

$$x^* = \frac{\mu - a}{\mu + b}$$

is stable; if

$$\mu > \frac{3a + b + \sqrt{(9a+b)(a+b)}}{2}, \ \left| f'\left(\frac{\mu - a}{\mu + b} \right) \right| = \left| \frac{ab + 2a\mu - \mu^2}{(a+b)\mu} \right| > 1,$$

the fixed point

$$x^* = \frac{\mu - a}{\mu + b}$$

is unstable.

This completes the proof.

2.2. Transcritical bifurcation and period-doubling bifurcation

With the discussion in Section 2.1, it can be found that the stability of the fixed point $x^* = 0$ can be changed at $\mu = a$, so the bifurcation maybe happen at $\mu = a$.

Lemma 1. *[24] Considering the one-parameter family of* C^r $(r \geq 2)$, *the one-dimensional map* $x \mapsto f(x, \mu)$, $x \in \mathbb{R}^1, \mu \in \mathbb{R}^1$, *if it satisfies*

$$f(0,0)=0,\ \frac{\partial f(0,0)}{\partial x}=1,\ \frac{\partial f}{\partial \mu}(0,0)=0,\ \frac{\partial^2 f}{\partial x\partial \mu}(0,0)\neq 0,\ \frac{\partial^2 f}{\partial x^2}(0,0)\neq 0,$$

then, the map undergoes a transcritical bifurcation at $(x,\mu)=(0,0)$.

According to Lemma 1, we have Theorem 2.

Theorem 2. *If* $\mu=a$, *the one-dimensional discrete system with three parameters and a square term* (3) *undergoes a transcritical bifurcation at the fixed point* $x^*=0$.

Proof of Theorem 2. Considering the fixed point $x^*=0$, the parameter $\mu=a$, let $\bar{\mu}=\mu-a$. We consider the parameter $\bar{\mu}$ as a new and dependent variable, then the one-dimensional discrete system with three parameters and a square term (3) becomes

$$x_{n+1}=h(x_n)=\frac{(\bar{\mu}+a)x_n(1-x_n)}{a+bx_n}. \tag{8}$$

Equation (8) can be described as

$$x\mapsto h(x,\bar{\mu})=\frac{(\bar{\mu}+a)x(1-x)}{a+bx}, \tag{9}$$

where $h(0,0)=0$.

With a simple calculation, we can obtain

$$\begin{aligned}
&\frac{\partial h(0,0)}{\partial x}=\frac{(\bar{\mu}+a)(a-2ax-bx^2)}{(a+bx)^2}\Big|_{(0,0)}=1,\\
&\frac{\partial h(0,0)}{\partial \bar{\mu}}=\frac{(x-x^2)}{a+bx}\Big|_{(0,0)}=0,\\
&\frac{\partial^2 h(0,0)}{\partial x^2}=\frac{-2(\bar{\mu}+a)(a+bx)^2-2b(\bar{\mu}+a)(a-2ax-bx^2)}{(a+bx)^3}\Big|_{(0,0)},\\
&\qquad=\frac{-2(a+b)}{a}\neq 0,\\
&\frac{\partial^2 h(0,0)}{\partial x\partial \bar{\mu}}=\frac{a-2ax-bx^2}{(a+bx)^2}\Big|_{(0,0)}=1\neq 0.
\end{aligned}$$

According to Lemma 1, the map (9) undergoes a transcritical bifurcation at $(x,\bar{\mu})=(0,0)$. It is equal to when the one-dimensional discrete system with three parameters and a square term (3) undergoes a transcritical bifurcation at $(x^*,\mu)=(0,a)$.

This completes the proof.

From Theorem 1, the stability of the fixed point

$$x^*=\frac{\mu-a}{\mu+b}$$

can be changed at

$$\mu = \frac{3a+b+\sqrt{(9a+b)(a+b)}}{2}.$$

Thus, the bifurcations may happen at

$$\mu = \frac{3a+b+\sqrt{(9a+b)(a+b)}}{2}.$$

Lemma 2. *[24] Consider a one-parameter family of* $C^r(r \geq 3)$, *the one-dimensional map* $x \mapsto f(x,\mu), x \in \mathbb{R}^1, \mu \in \mathbb{R}^1$, *if it satisfies*

$$f(0,0)=0,\ \frac{\partial f}{\partial x}(0,0)=-1,\ \frac{\partial f^2}{\partial \mu}(0,0)=0,\ \frac{\partial^2 f^2}{\partial x^2}(0,0)=0,\ \frac{\partial^2 f^2}{\partial x \partial \mu}(0,0)\neq 0,\ \frac{\partial^3 f^2}{\partial x^3}(0,0)\neq 0,$$

then the map undergoes a period-doubling bifurcation at $(x,\mu)=(0,0)$.

Theorem 3. *If*

$$\mu = \frac{3a+b+\sqrt{(9a+b)(a+b)}}{2},$$

one-dimensional discrete system with three parameters and a square term (3) *undergoes a period-doubling bifurcation at the fixed point*

$$x^* = \frac{\mu - a}{\mu + b}.$$

Proof of Theorem 3. Considering the parameter

$$\mu = \frac{3a+b+\sqrt{(9a+b)(a+b)}}{2},$$

the fixed point

$$x^* = \frac{\mu-a}{\mu+b} = \frac{a+b+\sqrt{(9a+b)(a+b)}}{3(a+b)+\sqrt{(9a+b)(a+b)}}.$$

Let

$$\bar{\mu} = \mu - \frac{3a+b+\sqrt{(9a+b)(a+b)}}{2},\ \ \bar{x}_n = x_n - x^*.$$

We consider the parameter $\bar{\mu}$ as a new and dependent variable, then the one-dimensional discrete system with three parameters and a square term (3) becomes

$$\begin{aligned}\bar{x}_{n+1} &= h(\bar{x}_n, \bar{\mu}) \\ &= \frac{\left(\bar{\mu} + \frac{3a+b+\sqrt{(9a+b)(a+b)}}{2}\right)\left[-\bar{x}_n^2 + (1-2x^*)\bar{x}_n + x^* - (x^*)^2\right] - ax^* - b\bar{x}_n x^* - b(x^*)^2}{a + b(\bar{x}_n + x^*)}.\end{aligned} \tag{10}$$

Equation (10) can be described as

$$\bar{x} \mapsto h(\bar{x}, \bar{\mu})$$
$$= \frac{\left(\bar{\mu} + \frac{3a+b+\sqrt{(9a+b)(a+b)}}{2}\right)\left[-\bar{x}^2 + (1-2x^*)\bar{x} + x^* - (x^*)^2\right] - ax^* - b\bar{x}\,x^* - b(x^*)^2}{a + b(\bar{x} + x^*)}, \tag{11}$$

where $h(0,0) = 0$. With a simple calculation, we can obtain

$$\frac{\partial h(0,0)}{\partial \bar{x}} = -1,$$

$$\frac{\partial^2 h^2(0,0)}{\partial \bar{x}^2} = 0,$$

$$\frac{\partial^2 h^2(0,0)}{\partial \bar{x}\partial \bar{\mu}}$$
$$= \frac{(432a^3 + 576a^2b + 192ab^2 + 16b^3)\sqrt{(9a+b)(a+b)} + 1296a^4 + 2448a^3b + 1408a^2b^2 + 272ab^3 + 16b^4}{[3a+b+\sqrt{(9a+b)(a+b)}]^4(a+b)}$$

$$\neq 0,$$

$$\frac{\partial^3 h^2(0,0)}{\partial x^3}$$
$$= -\left[\begin{array}{l} 81a^4 + 144a^3b + 27a^3\sqrt{(9a+b)(a+b)} + 80a^2b^2 + 33a^2b\sqrt{(9a+b)(a+b)} + 16ab^3 + \\ 11ab^2\sqrt{(9a+b)(a+b)} + b^4 + b^3\sqrt{(9a+b)(a+b)} \end{array}\right]$$
$$\times 12a\left[3a + 3b + \sqrt{(9a+b)(a+b)}\right]^4$$
$$/\left[(a+b)^3(9a^2 + 8ab + 3a\sqrt{(9a+b)(a+b)} + b^2 + b\sqrt{(9a+b)(a+b)})(3a+b+\sqrt{(9a+b)(a+b)})^4\right]$$
$$\neq 0.$$

According to Lemma 2, the map (11) undergoes a period-doubling bifurcation at

$$(\bar{x}, \bar{\mu}) = (0,0).$$

It is equal to when the one-dimensional discrete system with three parameters and a square term (3) undergoes a period-doubling bifurcation at

$$(x^*, \mu) = \left(\frac{a+b+\sqrt{(9a+b)(a+b)}}{3(a+b)+\sqrt{(9a+b)(a+b)}}, \frac{3a+b+\sqrt{(9a+b)(a+b)}}{2}\right).$$

This completes the proof.

2.3. Numerical experiments on stability and bifurcation

In this section, some numerical experiments are conducted to verify the correctness of the theoretical analysis of stability and bifurcation of the one-dimensional discrete system with three parameters and a square term (3).

When $a=1, b=0$, the one-dimensional discrete system with three parameters and a square term (3) is described as

$$x \mapsto f(x) = \mu x(1-x),$$

which is the logistic map. To investigate the evolution characteristics of the logistic map's iterative behavior across varying intervals of parameter μ, numerical experiments are conducted with the initial state $x_0 = 0.01$. The varying interval of parameter μ is set to $(0,4]$. In the experiment, the logistic map is iterated 500 times. The results of the first 200 iterations are discarded, and the subsequent 300 iterations' results are plotted. The numerical experiment result is shown in Figure 1. In Figure 1, when $0<\mu<1$, $x=0$, it means that the logistic map converges to $x^*=0$, and $x^*=0$ is a stable fixed point as $0<\mu<1$. When $1<\mu<3$, the logistic map converges to a non-zero state rather than to zero. This shows that the logistic map undergoes a transcritical bifurcation at

$$(x^*, \mu) = (0,1).$$

In Figure 1, it can be readily observed that $\mu=3$ is a critical value of the parameter for the logistic map. The logistic map undergoes a period-doubling bifurcation at $\mu=3$. The findings from the numerical experiments are consistent with the conclusions drawn from the theoretical analysis.

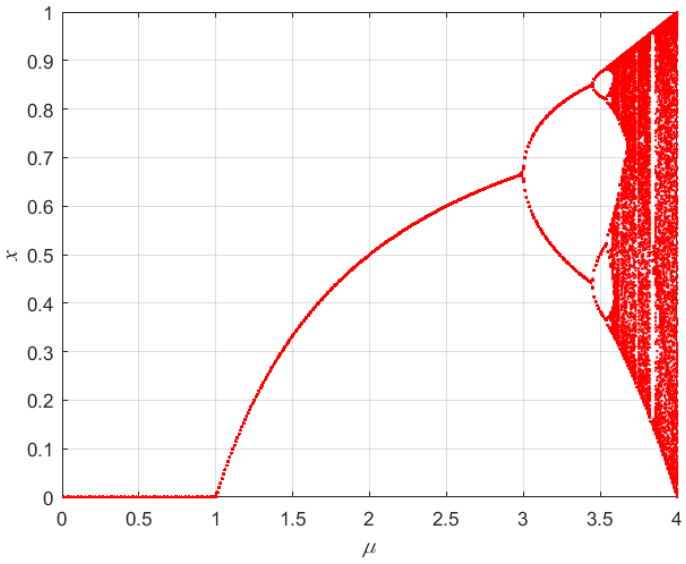

Figure 1. The output of x with respect to μ for the logistic map.

When $a=1, b=1$, the one-dimensional discrete system with three parameters and a square term (3) is described as

$$x \mapsto K(x) = \frac{\mu x(1-x)}{1+x},$$

which is the chaotic map K. To investigate the evolution characteristics of the chaotic map K's iterative behavior across varying intervals of parameter μ, numerical experiments are conducted with the initial state $x_0 = 0.01$. The varying interval of parameter μ is set to $(0,6]$. In the experiment, the chaotic map K is iterated 500 times. The results of the first 200 iterations are

discarded, and the subsequent 300 iterations' results are plotted. Figure 2 shows the output of x with respect to μ for $a=1, b=1$. In Figure 2, when $0<\mu<1, x=0$, it means that the chaotic map K converges to $x^*=0$, and $x^*=0$ is a stable fixed point as $0<\mu<1$. When

$$1<\mu<2+\sqrt{5},$$

the chaotic map K converges to a non-zero state rather than to zero. This means that the fixed point $x^*=0$ loses its stability as $\mu>1$. Thus, the chaotic map K undergoes a transcritical bifurcation at

$$(x^*,\mu)=(0,1).$$

In Figure 2, it can be readily observed that

$$\mu=2+\sqrt{5}$$

is a critical value of the parameter for the chaotic map K. The chaotic map K undergoes a period-doubling bifurcation at

$$\mu=2+\sqrt{5}.$$

From Figure 2, the findings from the numerical experiments are consistent with the results of [4]. This shows that the theoretical analysis is correct.

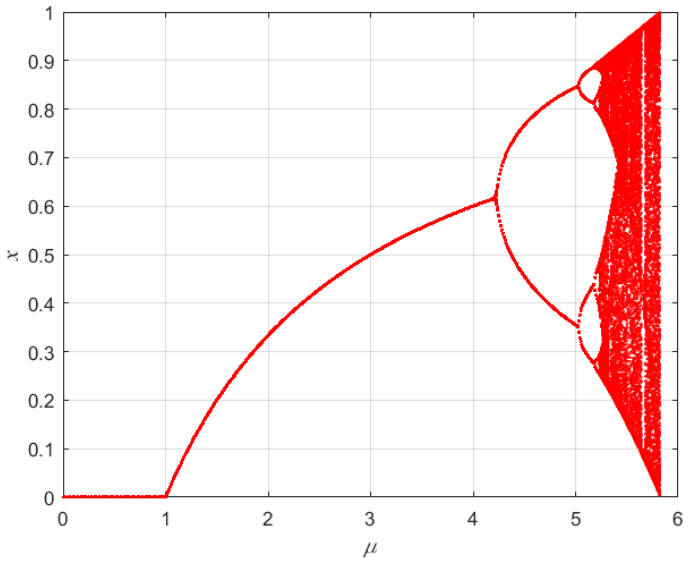

Figure 2. The output of x with respect to μ for the chaotic map K.

When $a=2, b=0.2$, the one-dimensional discrete system with three parameters and a square term (3) is described as

$$x\mapsto f(x)=\frac{\mu x(1-x)}{2+0.2x}.$$

Numerical experiments are conducted with the initial state $x_0=0.01$. The varying interval of parameter μ is set to $(0,9]$. In the experiment, the one-dimensional discrete system with three parameters and a square term (3) with $a=2, b=0.2$ is iterated 500 times. The results of the first 200

iterations are discarded, and the subsequent 300 iterations' results are plotted. Figure 3 shows the output of x with respect to μ. This demonstrates that when $0 < \mu < 2$, the one-dimensional discrete system with three parameters and a square term (3) with $a = 2, b = 0.2$ converges to the fixed point $x^* = 0$, and $x^* = 0$ is stable. When $\mu > 2$, the one-dimensional discrete system with three parameters and a square term (3) with $a = 2, b = 0.2$ converges to a non-zero state rather than to zero. Thus, the one-dimensional discrete system with three parameters and a square term (3) with $a = 2, b = 0.2$ undergoes a transcritical bifurcation at

$$(x^*, \mu) = (0, 2).$$

In Figure 3, it can be readily observed that the one-dimensional discrete system with three parameters and a square term (3) with $a = 2, b = 0.2$ undergoes a period-doubling bifurcation at

$$\mu = \frac{3a + b + \sqrt{(9a + b)(a + b)}}{2} \approx 6.26.$$

The results of the numerical experiments are consistent with the results of the theoretical analysis.

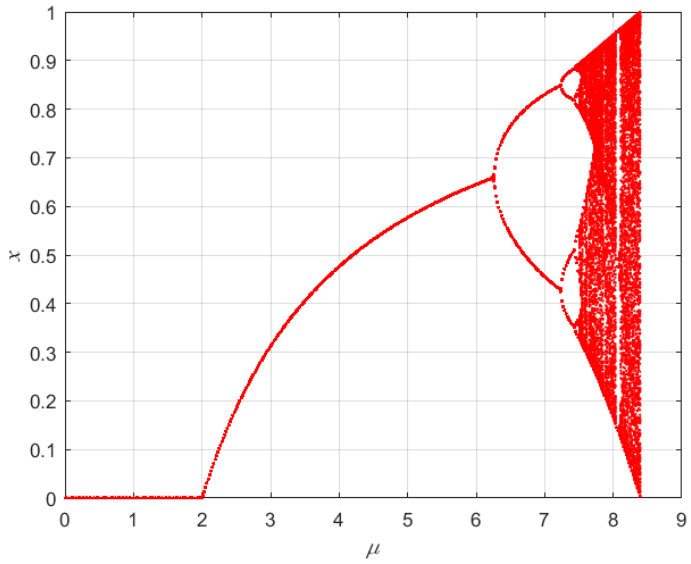

Figure 3. The output of x with respect to μ for the one-dimensional discrete system with three parameters and a square term (3) as $a = 2, b = 0.2$.

3. Anti-control of period-doubling bifurcation for the one-dimensional discrete system with three parameters and a square term

3.1. Linear feedback controller

Period-doubling bifurcation serves as a mechanism through which chaotic behavior can emerge. Therefore, in certain scenarios, the premature occurrence of period-doubling bifurcation may be necessary to facilitate the onset of chaos. The anti-controller of the period-doubling bifurcation can cause the premature occurrence of period-doubling bifurcation. Thus, in this section, we design an anti-controller of period-doubling bifurcation to make the one-dimensional discrete system with

three parameters and a square term (3) to undergo the period-doubling bifurcation at a predetermined parameter's position, and the period-doubling bifurcation point appears in the period-1 orbit.

Considering the one-dimensional discrete system with three parameters and a square term (3), the controlled system of anti-controlling of period-doubling bifurcation is taken as

$$x_{n+1} = \overline{f}(x_n) = \frac{\mu x_n(1-x_n)}{a+bx_n} + u, \tag{12}$$

where u is a linear feedback controller, which is designed as

$$u = k_1 + k_2 x_n, \tag{13}$$

k_1 and k_2 are control parameters. Substituting feedback controller (13) into system (12), controlled system (12) can be described as

$$x_{n+1} = \overline{f}(x_n) = \frac{\mu x_n(1-x_n)}{a+bx_n} + k_1 + k_2 x_n. \tag{14}$$

According to Theorem 1, when

$$\mu \in (a, \frac{3a+b+\sqrt{(9a+b)(a+b)}}{2}),$$

the equality

$$x^* = \frac{\mu - a}{\mu + b}$$

is the period-1 point of the one-dimensional discrete system with three parameters and a square term (3), and the one-dimensional discrete system with three parameters and a square term (3) is stable at

$$x^* = \frac{\mu - a}{\mu + b}.$$

Thus, the one-dimensional discrete system with three parameters and a square term (3) cannot undergo the period-doubling bifurcation at μ, where

$$\mu \in (a, \frac{3a+b+\sqrt{(9a+b)(a+b)}}{2}).$$

In order to make the period-doubling bifurcation of the one-dimensional discrete system with three parameters and a square term (3) come out in advance, and make the period-doubling bifurcation point appear in the period-1 orbit, we choose the predetermined parameter's position to be $\mu = \mu_0$, and

$$\mu_0 \in (a, \frac{3a+b+\sqrt{(9a+b)(a+b)}}{2}).$$

With the anti-controller of period-doubling bifurcation, we choose the proper control parameters k_1 and k_2 to generate the period-doubling bifurcation at μ_0, and make

$$x^* = \frac{\mu_0 - a}{\mu_0 + b}$$

to be the period-1 point of the controlled system (14). Moreover, the controlled system (14) is stable at

$$x^* = \frac{\mu_0 - a}{\mu_0 + b}.$$

According to the above analysis, the processes of determining the proper control parameters k_1 and k_2 are listed as follows:

a) Control parameters k_1 and k_2 are needed to make

$$x^* = \frac{\mu_0 - a}{\mu_0 + b}$$

to be the period-1 point of the controlled system (14).

In order to make

$$x^* = \frac{\mu_0 - a}{\mu_0 + b}$$

to be the period-1 point of the controlled system (14), $\frac{\mu_0 - a}{\mu_0 + b}$ must satisfy

$$\frac{\mu_0 - a}{\mu_0 + b} = \frac{\mu_0\left(\frac{\mu_0 - a}{\mu_0 + b}\right)\left(1 - \frac{\mu_0 - a}{\mu_0 + b}\right)}{a + b\left(\frac{\mu_0 - a}{\mu_0 + b}\right)} + k_1 + k_2\left(\frac{\mu_0 - a}{\mu_0 + b}\right). \tag{15}$$

With a simple calculation, k_1 and k_2 satisfy

$$k_1 + k_2\frac{\mu_0 - a}{\mu_0 + b} = 0. \tag{16}$$

b) Control parameters k_1 and k_2 are needed to guarantee the controlled system (11) is stable at the fixed point

$$x^* = \frac{\mu_0 - a}{\mu_0 + b}.$$

In order to have a controlled system (14) be stable at

$$x^* = \frac{\mu_0 - a}{\mu_0 + b},$$

it must have

$$\left|\overline{f}'(\frac{\mu_0-a}{\mu_0+b})\right|<1.$$

Since the Jacobi matrix of controlled system (14) at the fixed point

$$x^*=\frac{\mu_0-a}{\mu_0+b}$$

is

$$\overline{f}'(\frac{\mu_0-a}{\mu_0+b})=\frac{-\mu_0^2+2a\mu_0+ab}{(a+b)\mu_0}+k_2,$$

thus k_1 and k_2 must satisfy

$$\left|\frac{-\mu_0^2+2a\mu_0+ab}{(a+b)\mu_0}+k_2\right|<1. \tag{17}$$

c) Control parameters k_1 and k_2 are needed to ensure that the controlled system (14) has period-2 points.

In the controlled system (14), period-2 points x must satisfy

$$x=\overline{f}(\overline{f}(x)). \tag{18}$$

That is

$$x=\frac{\mu_0[\frac{\mu_0x(1-x)}{a+bx}+k_1+k_2x]\cdot[1-\frac{\mu_0x(1-x)}{a+bx}-k_1-k_2x]}{a+b[\frac{\mu_0x(1-x)}{a+bx}+k_1+k_2x]}+k_1+k_2[\frac{\mu_0x(1-x)}{a+bx}+k_1+k_2x]. \tag{19}$$

Four analytical solutions of Eq (19) are

$$x_1=\frac{-bk_1-ak_2-\mu_0+a+\sqrt{\mu_0^2+(4k_1a+2ak_2+2bk_1-2a)\mu_0+(ak_2-bk_1-a)^2}}{(2k_2-2)b-2\mu_0},$$

$$x_2=\frac{-bk_1-ak_2-\mu+a-\sqrt{\mu_0^2+(4k_1a+2ak_2+2bk_1-2a)\mu_0+(ak_2-bk_1-a)^2}}{(2k_2-2)b-2\mu_0},$$

$$\sqrt{\left\{\begin{array}{l}k_1^2(k_2+1)b^3-2k_1[(\frac{k_1}{2}-k_2-1)\mu_0+a(k_2^2-1)]b^2\\+[(-2k_1+k_2+1)\mu_0^2+6a(k_1k_2+\frac{1}{3}k_2^2+\frac{1}{3}k_1+\frac{1}{3})\mu_0\\+a^2(k_2+1)(k_2-1)^2]b-[\mu_0^2+4a(k_1+\frac{k_2}{2}-\frac{1}{2})\mu_0\\+a^2(k_2+1)(k_2-3)]\mu_0\end{array}\right\}\cdot(k_2b+b-\mu_0)}$$

$$x_3=\frac{-(k_1k_2+k_1)b^2+[(k_1-k_2-1)\mu_0-ak_2^2-2ak_2-a]b+\mu_0^2+(ak_2+a)\mu_0}{2(bk_2-\mu_0)[(k_2+1)b-\mu_0]},$$

$$-\sqrt{\left\{\begin{array}{l} k_1^2(k_2+1)b^3-2k_1[(\frac{k_1}{2}-k_2-1)\mu_0+a(k_2^2-1)]b^2 \\ +[(-2k_1+k_2+1)^2\mu_0^2+6a(k_1k_2+\frac{1}{3}k_2^2+\frac{1}{3}k_1+\frac{1}{3})\mu_0 \\ +a^2(k_2+1)(k_2-1)^2]b-[\mu_0^2+4a(k_1+\frac{k_2}{2}-\frac{1}{2})\mu_0 \\ +a^2(k_2+1)(k_2-3)]\mu_0 \end{array}\right\}\cdot(k_2b+b-\mu_0)}$$

$$x_4=\frac{-(k_1k_2+k_1)b^2+[(k_1-k_2-1)\mu_0-ak_2^2-2ak_2-a]b+\mu_0^2+(ak_2+a)\mu_0}{2(bk_2-\mu_0)[(k_2+1)b-\mu_0]}.$$

After calculation, x_3 and x_4 are the period-2 points of the controlled system (14), x_1 and x_2 are the period-1 points of the controlled system (14).

To ensure that the periodic points x_3 and x_4 are real numbers, k_1 and k_2 must satisfy

$$\left\{\begin{array}{l} k_1^2(k_2+1)b^3-2k_1[(\frac{k_1}{2}-k_2-1)\mu_0+a(k_2^2-1)]b^2 \\ +[(-2k_1+k_2+1)\mu_0^2+6a(k_1k_2+\frac{1}{3}k_2^2+\frac{1}{3}k_1+\frac{1}{3})\mu_0+a^2(k_2+1)(k_2-1)^2]b \\ -[\mu_0^2+4a(k_1+\frac{k_2}{2}-\frac{1}{2})\mu_0+a^2(k_2+1)(k_2-3)]\mu_0 \end{array}\right\}\cdot(k_2b+b-\mu_0)\geq 0 \quad (20)$$

and

$$2(bk_2-\mu_0)(k_2b+b-\mu_0)\neq 0\,. \quad (21)$$

Combining the above analysis, we obtain Theorem 4.

Theorem 4. *For the one-dimensional discrete system with three parameters and a square term* (3), *the anti-controller of period-doubling bifurcation is designed as*

$$u=k_1+k_2x_n\,.$$

Let the predetermined parameter's position be μ_0, *and*

$$\mu_0\in(a,\frac{3a+b+\sqrt{(9a+b)(a+b)}}{2})\,.$$

If the control parameters k_1 *and* k_2 *meet the following conditions*:

$$\begin{cases} k_1 + k_2 \dfrac{\mu_0 - a}{\mu_0 + b} = 0, \\ \left| \dfrac{-{\mu_0}^2 + 2a\mu_0 + ab}{(a+b)\mu_0} + k_2 \right| < 1, \\ \left[\begin{array}{l} k_1^2(k_2+1)b^3 - 2k_1[(\dfrac{k_1}{2} - k_2 - 1)\mu_0 + a(k_2^2 - 1)]b^2 + [(-2k_1 + k_2 + 1){\mu_0}^2 \\ +6a(k_1k_2 + \dfrac{1}{3}k_2^2 + \dfrac{1}{3}k_1 + \dfrac{1}{3})\mu_0 + a^2(k_2+1)(k_2-1)^2]b - \\ [{\mu_0}^2 + 4a(k_1 + \dfrac{k_2}{2} - \dfrac{1}{2})\mu_0 + a^2(k_2+1)(k_2-3)]\mu_0 \end{array} \right] \cdot (k_2 b + b - \mu_0) \geq 0, \\ 2(bk_2 - \mu_0)(k_2 b + b - \mu_0) \neq 0, \end{cases} \tag{22}$$

the discrete system (3) *with the anti-controller of period-doubling bifurcation undergoes a period-doubling bifurcation at*

$$(x^*, \mu) = (\frac{\mu_0 - a}{\mu_0 + b}, \mu_0),$$

and the period-doubling bifurcation point appears in the period-1 *orbit*.

3.2. Numerical experiments on anti-control of period-doubling bifurcation

3.2.1. Effectiveness and robustness of the anti-controller of period-doubling bifurcation

In this section, we do some numerical experiments to test the effectiveness of the anti-controller of period-doubling bifurcation for the one-dimensional discrete system with three parameters and the square term (3).

When $a = 1, b = 1$, the one-dimensional discrete system with three parameters and a square term (3) is the chaotic map K. In order to investigate the dynamical behavior and the chaotic degree of the strange attractors, numerical experiments are conducted to evaluate the Lyapunov exponents with varying parameter μ. The numerical experiments' results are listed in Figure 4. Figure 4 is the Lyapunov exponent diagram of the chaotic map K with the initial state $x_0 = 0.01$ and the varying interval of parameter μ to be $[1, 5.5]$.

From the Figure 4, we learn that the Lyapunov exponents are negative with $1 \leq \mu < 5.23$, and the Lyapunov exponents are positive with $5.23 \leq \mu \leq 5.5$. This means that the chaotic map K is stable as $1 \leq \mu < 5.23$, and the chaotic map K is chaotic as $5.23 \leq \mu \leq 5.5$. Thus, the chaotic map K occurs the chaotic phenomenon once μ exceeds the value 5.23. In order to make the chaotic phenomenon occur in advance, the anti-controller of the period-doubling bifurcation is applied to chaotic map K. From Figure 2, the chaotic map undergoes the period-doubling bifurcation at $\mu = 2 + \sqrt{5}$. In order to make the period-doubling bifurcation occur in advance, we set the predetermined parameter's position to be $\mu_0 = 2$. When $a = 1, b = 1, \mu_0 = 2$, the control parameters k_1 and k_2 are computed using formula (22). The results of k_1 and k_2 are $k_1 = 0.416$, $k_2 = -1.249$. Chaotic map K with the anti-controller of the period-doubling bifurcation is described as

$$x_{n+1} = \frac{\mu x_n (1 - x_n)}{1 + x_n} + 0.416 - 1.249 x_n . \tag{23}$$

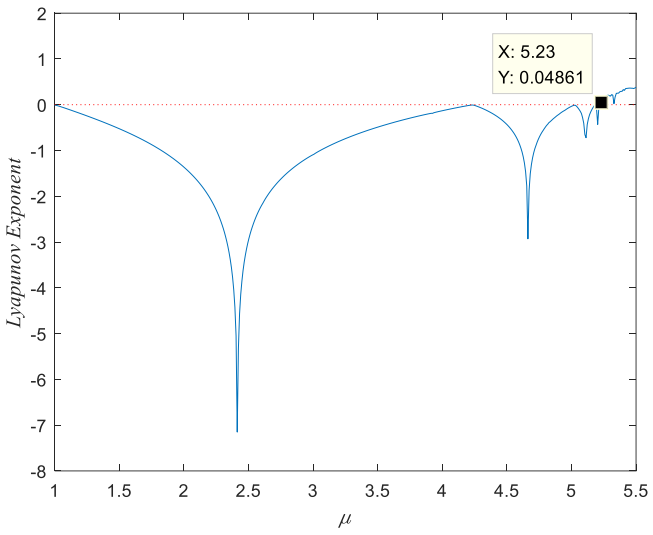

Figure 4. Lyapunov exponent diagram of chaotic map K without controllers.

Numerical simulations are conducted to investigate the iterative behavior of the system (23) across varying intervals of parameter μ. The varying interval of parameter μ is set to $[1, 4.5]$, and the initial state is $x_0 = 0.01$. In the experiment, system (23) is iterated 500 times. The results of the first 100 iterations are discarded, and the subsequent 400 iterations' results are plotted. The numerical simulation's results are shown in Figure 5.

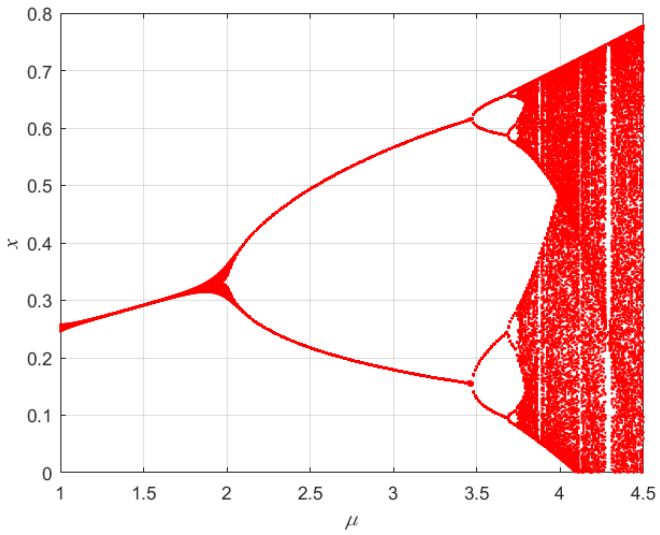

Figure 5. Bifurcation diagram of x vs. μ for chaotic map K with the anti-controller of the period-doubling bifurcation.

It is obvious that chaotic map K with the anti-controller of the period-doubling bifurcation undergoes a period-doubling bifurcation at $\mu = 2$. The anti-controller of the period-doubling

bifurcation is effective. Figure 6 is the Lyapunov exponent diagram of the controlled system (23) with $k_1 = 0.416, k_2 = -1.249$. This shows that the chaotic phenomenon occurs as $\mu = 3.744$. The purpose of making chaos appear in advance has been achieved.

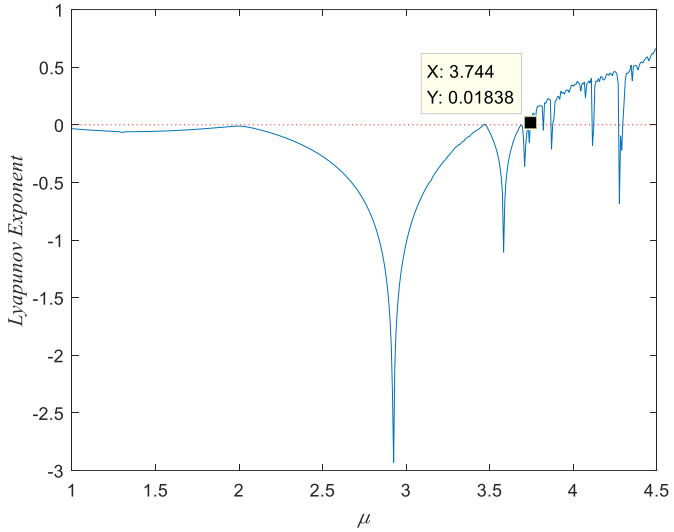

Figure 6. Lyapunov exponent diagram of chaotic map K with the anti-controller of the period-doubling bifurcation.

For the numerical experiment of Figure 5, we set a perturbation $\Delta x = 0.1$ to the initial state $x_0 = 0.01$. Figure 7 is the bifurcation diagram of the controlled system (23) with varying intervals of parameter μ and the initial state $x_0 = 0.11$. In Figure 7, the period-doubling bifurcation still occurs at $\mu = 2$ for the controlled system (23). This indicates that the anti-controller of period-doubling bifurcation is robust.

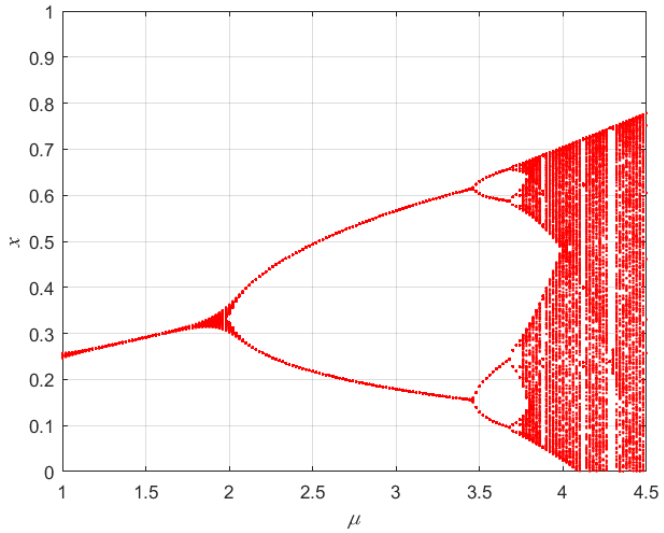

Figure 7. Bifurcation diagram of x vs. μ for chaotic map K with the anti-controller of the period-doubling bifurcation, where initial states $x_0 = 0.11$, $k_1 = 0.416$, and $k_2 = -1.249$.

3.2.2. Application of the anti-control of period-doubling bifurcation in image encryption

From Section 3.2.1, it is indicated that the anti-controller of period-doubling bifurcation can make the chaos appear in advance. The chaotic sequence generated via period-doubling bifurcation exhibits a high degree of randomness and unpredictability, making it suitable for image encryption. Given that chaotic sequences frequently emerge near period-doubling bifurcations, when the system lacks chaotic behavior, a predetermined parameter's position can be established within the range of period-1 of the system. By anti-control of period-doubling bifurcation, period-doubling bifurcations can be induced at specified predetermined parameter points. Subsequently, parameter values in the vicinity of the period-doubling bifurcation are incorporated into the image encryption algorithm, enabling the system to generate complex chaotic dynamics through the period-doubling process as parameters evolve. This approach facilitates the generation of pseudo-random sequences for pixel position permutation or pixel gray value encryption, thereby enhancing image encryption effectiveness.

In this section, anti-control of period-doubling bifurcation for the one-dimensional discrete system with three parameters and a square term (3) is used in image encryption. In order to illustrate how to use the anti-controller of period-doubling control in image encryption, we take chaotic map K as an example. In Section 3.2.1, chaotic map K with an anti-controller of the period-doubling bifurcation undergoes the period-doubling bifurcation at $\mu = 2$. Thus, controlled chaotic map K is used in image encryption, in which the plaintext image is "Lena",

$$k_1 = 0.416, \quad k_2 = -1.249, \quad 2 \le \mu \le 4.6,$$

and the initial state $x_0 = 0.01$. In the numerical experiment, chaotic map K is iterated 5000 times for every $\mu \in [2, 4.6]$. The results of the first 1000 iterations are discarded, and the subsequent 4000 iterations' results are used in image encryption. Figure 8 lists the plaintext image, the encryption image, and the decryption image.

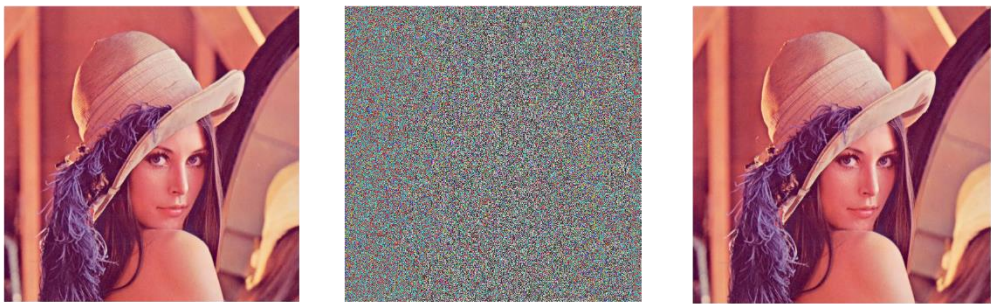

(a) plaintext image (b) ciphertext image (c) decryptionb image

Figure 8. The correlation diagram of the image encryption using chaotic map K with the anti-controller of period-doubling bifurcation.

This shows that image encryption with anti-control of period-doubling bifurcation is effective. Table 1 lists the R-channel correlations of plaintext image and ciphertext image. Table 2 lists the G-channel correlations of plaintext image and ciphertext image. Table 3 lists the B-channel correlations of plaintext image and ciphertext image. The lower the correlation between adjacent

pixels in a ciphertext image, the greater the resistance of the encryption algorithm to statistical analysis attacks. As the correlation coefficient of adjacent pixels in the ciphertext image approaches zero, the security of the encryption scheme is significantly enhanced. From Table 1 to Table 3, the correlation coefficients of the ciphertext image all approach zero. This means that the image encryption with anti-control of period-doubling bifurcation works very well. The information entropy of an image quantifies the unpredictability of the pixel gray-level distribution. For a grayscale image, the theoretical maximum information entropy is 8. A higher information entropy in the encrypted image indicates enhanced security of the ciphertext image. Table 4 lists the information entropy of the "Lena" ciphertext images with different discrete maps [25–28]. The information entropy of them is very close to 8. The number of pixel change rate (NPCR) and the unified average changing intensity (UACI) are two critical metrics employed to evaluate the robustness against differential attacks. Table 5 lists NPCR and UACI of image encryption with different discrete maps. It is obvious that NPCR and UACI of image encryption using chaotic map K with anti-controller of period-doubling bifurcation is a little larger than the other maps. Thus, the image encryption using chaotic map K with an anti-controller of period-doubling bifurcation demonstrates superior resistance to differential attacks.

Table 1. R-channel correlation.

	Horizontal correlation	Vertical correlation	Diagonal correlation
Plaintext image R-channel correlation	0.97433	0.98846	0.96517
Ciphertext image R-channel correlation	-0.0078077	-0.012912	-0.021584

Table 2. G-channel correlation.

	Horizontal correlation	Vertical correlation	Diagonal correlation
Plaintext image G-channel correlation	0.97416	0.98934	0.96534
Ciphertext image G-channel correlation	0.010953	-0.02186	0.0074832

Table 3. B-channel correlation.

	Horizontal correlation	Vertical correlation	Diagonal correlation
Plaintext image B-channel correlation	0.94955	0.97574	0.9342
Ciphertext image B-channel correlation	-0.010818	-0.0065805	0.0037925

Table 4. Information entropy test results.

Discrete map	R	G	B
The chaotic map K with anti-controller of period-doubling bifurcation	7.9992	7.9993	7.9992
Ref. [25]	7.9993	7.9992	7.9993
Ref. [26]	7.9994	7.9994	7.9994
Ref. [27]	7.9994	7.9994	7.9993
Ref. [28]	7.9992	7.9993	7.9993

Table 5. NPCR and UACI.

Discrete map	NPCR (%)	UACI (%)
The chaotic map K with anti-controller of period-doubling bifurcation	99.613	30.428
Ref. [25]	99.615	30.427
Ref. [26]	99.607	30.388
Ref. [27]	99.608	30.424
Ref. [28]	99.614	30.42

4. Conclusions

The main work of this paper includes three contents. The first content proposes the one-dimensional discrete system with three parameters and a square term (3), which are defined as

$$x_{n+1} = f\left(x_n\right) = \frac{\mu x_n (1 - x_n)}{a + b x_n}, \quad n = 0, 1, 2, \ldots .$$

The logistic map and chaotic map K both belong to the one-dimensional discrete system with three parameters and a square term (3). The stability of the fixed points and the bifurcation characteristics of the one-dimensional discrete system with three parameters and a square term (3) are analyzed by theoretical analysis and numerical experiments in this paper. Moreover, the existence conditions of period-doubling bifurcation are derived in this paper.

The second content is designing the anti-controller of period-doubling bifurcation for the one-dimensional discrete system with three parameters and a square term (3). By using the analytic method and the numerical computation, the proper control parameters of the anti-controller of period-doubling bifurcation are determined. With the adjustment of the control parameters, period-doubling bifurcation can generate at a predetermined position. The linear state feedback anti-controller of period-doubling bifurcation is effective and has robustness.

The third content uses the anti-controller of period-doubling bifurcation of the one-dimensional discrete system with three parameters and a square term (3) to realize image encryption. Comparative experiments show that this method is effective in image encryption.

The paper not only supplements the research of one-dimensional discrete systems with three parameters and a square term (3) but also has important theoretical value for one-dimensional discrete systems. The design idea of the anti-controller of period-doubling bifurcation can widely be extended to study two-dimensional maps or high-dimensional maps.

Author contributions

Limei Liu: conceptualization, methodology, software, validation, writing—original draft preparation, writing—review and editing; Xitong Zhong: conceptualization, methodology, software, validation, writing—original draft preparation, writing—review and editing. All authors have read and agreed to the published version of the manuscript.

Use of Generative-AI tools declarations

The authors declare they have not used Artificial Intelligence (AI) tools in the creation of this article.

Conflict of interest

All authors declare no conflicts of interest in this paper.

References

1. M. Chen, Pattern dynamics of a Lotka-Volterra model with taxis mechanism, *Appl. Math. Comput.*, **484** (2025), 129017. https://doi.org/10.1016/j.amc.2024.129017
2. M. Perc, Visualizing the attraction of strange attractors, *Eur. J. Phys.*, **26** (2005), 579–587. https://doi.org/10.1088/0143-0807/26/4/003
3. M. Ciobanu, A. Ardelean, C. Cotoraci, L. Mos, Maximum Lyapunov exponents evidencing chaos in neural activity, *J. Comput. Theor. Nanosci.*, **10** (2013), 2600–2603. https://doi.org/10.1166/jctn.2013.3255
4. A. Kumar, J. Alzabut, S. Kumari, M. Rani, R. Chugh, Dynamical properties of a novel one-dimensional chaotic map, *Math. Biosci. Eng.*, **19** (2022), 2489–2505. https://doi.org/10.3934/mbe.2022115
5. L. Moysis, M. Lawnik, M. S. Baptista, C. Volos, G. F. Fragulis, A family of 1D modulo-based maps without equilibria and robust chaos: application to a PRBG, *Nonlinear Dyn.*, **112** (2024), 12597–12621. https://doi.org/10.1007/s11071-024-09701-w
6. H. Litimi, A. BenSaida, L. Belkacem, O. Abdallah, Chaotic behavior in financial market volatility, *J. Risk*, **21** (2019), 27–53. https://doi.org/ 10.21314/JOR.2018.400
7. J. Belaire-Franch, Estimating the maximum Lyapunov exponent with denoised data to test for chaos in the German stock market, *Comput. Econ.*, 2024. https://doi.org/10.1007/s10614-024-10812-0
8. O. Benrhouma, A. B. Alkhodre, A. AlZahrani, A. Namoun, W. A. Bhat, Using singular value decomposition and chaotic maps for selective encryption of video feeds in smart traffic management, *Appl. Sci.*, **12** (2022), 3917. https://doi.org/10.3390/app12083917
9. L. Wang, L. Xu, G. Long, Y. Ma, J. Xiong, J. Wu, Visually secure traffic image encryption scheme using new two-dimensional Sigmoid-type memristive chaotic map and Laguerre transform embedding, *Phys. Scr.*, **99** (2024), 075266. https://doi.org/10.1088/1402-4896/ad54ff
10. M. K. Khairullah, A. A. Alkahtani, M. Z. B. Baharuddin, A. M. Al-Jubari, Designing 1D chaotic maps for fast chaotic image encryption, *Electronics*, **10** (2021), 2116. https://doi.org/10.3390/electronics10172116
11. Z. Hua, Z. Wu, Y. Zhang, H. Bao, Y. Zhou, Two-dimensional cyclic chaotic system for noise-reduced OFDM-DCSK communication, *IEEE Trans. Circuits Syst. I*, **72** (2025), 323–336. https://doi.org/10.1109/TCSI.2024.3454535
12. Y. Zhang, H. Xiang, S. Zhang, L. Liu, Construction of high-dimensional cyclic symmetric chaotic map with one-dimensional chaotic map and its security application, *Multimedia Tools Appl.*, **82** (2023), 17715–17740. https://doi.org/10.1007/s11042-022-14044-y

13. R. M. May, Simple mathematical models with very complicated dynamics, *Nature*, **261** (1976), 459–467. https://doi.org/10.1038/261459a0
14. Y. Zhou, L. Bao, C. P. Chen, A new 1D chaotic system for image encryption, *Signal Process.*, **97** (2014), 172–182. https://doi.org/10.1016/j.sigpro.2013.10.034
15. N. Khurana, M. Dua, A novel one-dimensional cosine within sine chaotic map and novel permutation-diffusion based medical image encryption, *Nonlinear Dyn.*, **113** (2025), 4839–4859. https://doi.org/10.1007/s11071-024-10429-w
16. L. F. Liu, J. Wang, A cluster of 1D quadratic chaotic map and its applications in image encryption, *Math. Comput. Simul.*, **204** (2023), 89–114. https://doi.org/10.1016/j.matcom.2022.07.030
17. X. Su, J. Wang, A. Bao, Stability analysis and chaos control in a discrete predator-prey system with Allee effect, fear effect, and refuge, *AIMS Math.*, **9** (2024), 13462–13491. https://doi.org/10.3934/math.2024656
18. B. Wang, Q. Zhu, Stability analysis of discrete-time semi-Markov jump linear systems, *IEEE Trans. Autom. Control*, **65** (2020), 5415–5421. https://doi.org/10.1109/TAC.2020.2977939
19. H. Kang, Y. Cong, G. Yan, Theoretical analysis of dynamic behaviors of cable-stayed bridges excited by two harmonic forces, *Nonlinear Dyn.*, **102** (2020), 965–992. https://doi.org/10.1007/s11071-020-05763-8
20. E. Zhu, M. Xu, D. Pi, Anti-control of hopf bifurcation for high-dimensional chaotic system with coexisting attractors, *Nonlinear Dyn.*, **110** (2022), 1867–1877. https://doi.org/10.1007/s11071-022-07723-w
21. Z. Wang, J. Qin, Anti-control of period-doubling bifurcation in cable-stayed beam, *J. Vib. Eng. Technol.*, **13** (2025), 18. https://doi.org/10.1007/s42417-024-01708-2
22. L. Zhang, J. Tang, K. Ouyang, Anti-control of period-doubling bifurcation for a variable substitution model of Logistic map, *Optik*, **130** (2017), 1327–1332. https://doi.org/10.1016/j.ijleo.2016.11.142
23. F. E. Smith, Population dynamics in daphnia magna and a new model for population growth, *Ecology*, **44** (1963), 651–663. https://doi.org/10.2307/1933011
24. S. Wiggins, *Introduction to applied nonlinear dynamical systems and chaos*, Springer Science Business Media, 1990. https://doi.org/10.1007/b97481
25. L. Liu, X. Zhong, Research on stability and bifurcation for two-dimensional two-parameter squared discrete dynamical systems, *Mathematics*, **12** (2024), 2423. https://doi.org/10.3390/math12152423
26. M. Benedicks, L. Carleson, The dynamics of the Hénon map, *Ann. Math.*, **133** (1991), 73–169. https://doi.org/10.2307/2944326
27. Y. Gao, Complex dynamics in a two-dimensional noninvertible map, *Chaos Solitons Fract.*, **39** (2009), 1798–1810. https://doi.org/10.1016/j.chaos.2007.06.051
28. B. Li, Q. He, Bifurcation analysis of a two-dimensional discrete Hindmarsh-Rose type model, *Adv. Differ. Equations*, **2019** (2019), 124. https://doi.org/10.1186/s13662-019-2062-z